

# AN ANALYSIS OF RESIDUAL STRESSES IN PIPELINE STEEL: A COMPARATIVE STUDY USING X-RAY DIFFRACTION AND ULTRASONIC TECHNIQUES

Bruna Machado<sup>1</sup>, Gabriela Ribeiro Pereira<sup>2</sup>, Maurício Motta<sup>3</sup> and Maria Cindra Fonseca<sup>1\*</sup>

<sup>1</sup>Department of Mechanical Engineering/PGMEC – UFF, Universidade Federal Fluminense, CEP 24210-346, Niterói-RJ, Brazil. E-mail: [mariacindra@id.uff.br](mailto:mariacindra@id.uff.br)

<sup>2</sup>Department of Metallurgical and Materials Engineering/COPPE, Universidade Federal do Rio de Janeiro-RJ, P.O. Box 68505, CEP 219415-972, Rio de Janeiro-RJ, Brazil. E-mail: [gpereira@metalmat.ufrj.br](mailto:gpereira@metalmat.ufrj.br)

<sup>3</sup>Department of Mechanical Engineering, CEFET/RJ, CEP 20271-110, Rio de Janeiro-RJ, Brazil. E-mail: [mmotta64@gmail.com](mailto:mmotta64@gmail.com)

## ABSTRACT

*The occurrence of residual stresses is inherent in all manufacturing processes, and under external loading, residual and applied stresses can linearly sum even in the elastic regime, leading to unexpected component failure. Therefore, offering alternative techniques that facilitate the qualification and quantification of residual stresses is a task of great significance. In this context, this study aims to provide a comparative study of residual stresses in samples of API X80 steel, using two non-destructive techniques: X-ray diffraction employing the  $\sin^2\psi$  method and ultrasonic testing utilizing the Rayleigh wave. The results demonstrate that the time of flight wave was consistent with the residual stresses measured through X-ray diffraction. The ultrasonic signals exhibited sensitivity to the nature and magnitude of the residual stresses. The comparative analysis provides valuable insights for the selection and application of non-destructive techniques in assessing residual stresses, contributing to the enhanced safety and performance of structures and components.*

**KEYWORDS:** residual stresses, X-ray diffraction, ultrasound, Rayleigh wave, API X80 steel.

## I. INTRODUCTION

The occurrence of residual stresses is inherent in all manufacturing processes, and under external loading, residual and applied stresses can linearly accumulate even within the elastic regime, leading to unexpected and premature component failure [1, 4]. Understanding the nature and magnitude of residual stresses in a component or structure is crucial for predicting the potential consequences of these stress fields. In some cases, the combination of compressive residual stresses with service stresses, even within the elastic regime, can result in premature failures.

It is well-established that tensile residual stresses are detrimental to the fatigue life of materials as they increase the risk of crack initiation and propagation. Additionally, tensile residual stresses can enhance the tendency for stress corrosion cracking. On the contrary, compressive residual stresses are beneficial as they can suppress crack nucleation and propagation, thereby improving the fatigue life of the material [2, 3]. Therefore, accurate measurement and management of residual stresses are essential for ensuring the safe and reliable operation of steel pipelines.

Several techniques, including X-ray and neutron diffraction, hole-drilling, ultrasound, and magnetic Barkhausen noise, can be employed to measure residual stresses. However, each technique has its own limitations and challenges [3-5]. In the case of ultrasound, despite numerous studies on its application for residual stress measurement, the accuracy of this technique is not yet well-established due to various factors that can influence the travel time of ultrasonic waves.

The results obtained from X-ray diffraction analysis revealed high tensile residual stresses in the API 5L-X80 steel samples, which can lead to a decrease in fatigue life and an increase in stress corrosion tendency [2-4]. Conversely, the ultrasound technique utilizing Rayleigh waves indicated the presence of compressive residual stresses in the samples, which can suppress crack nucleation and propagation, thereby enhancing the material's durability.

The analysis of residual stresses is crucial for evaluating the mechanical properties and durability of materials, particularly for those employed in critical applications such as large-diameter pipes for oil and gas transportation [5-7]. The combination of X-ray diffraction and ultrasound techniques can provide a more comprehensive understanding of the residual stress state in steels, facilitating improved design and maintenance decisions.

API 5LX80 steel is a high-strength low-alloy (HSLA) steel with a minimum yield strength of 80 ksi, making it suitable for use in pipelines for oil and gas transportation. However, during manufacturing, this steel may develop tensile or compressive residual stresses that can influence its mechanical properties and service life. Understanding the pattern and magnitude of these residual stresses is crucial for ensuring the integrity of the pipeline throughout its lifetime [8, 9].

This paper is organized as follows: Section I presents the introduction, addressing the importance of residual stress analysis in steel pipelines and complemented with a Table containing the state-of-art of application of ultrasonic technique. Section II describes the materials and methods used in the study, including information about the samples and the X-ray diffraction and ultrasonic techniques. Section III presents the results and discussions obtained from the performed analyses, with a particular focus on residual stress measurements. Section IV provides the conclusions of the study, highlighting the main contributions of research. Finally, Section V lists the references that supported this work.

Table 1 presents many publications about the state-of-art in the surface integrity studies by ultrasonic technique. This table provides valuable information regarding number of citations, objectives, and key findings of these studies.

**Table 1.** State-of-art: relationship between residual stress and ultrasonic technique.

Title	Authors	Year	Main conclusions
Assessment of Residual Stress by Ultrasonic Testing and Neutron Diffraction in Laser Beam Welded Aluminum Alloy [2].	Testa, G., Bonora, N., Gentile, D., Ruggiero, A., Iannitti, G., Carlucci, A., Madi, Y.	2017	The combination of ultrasonic testing and neutron diffraction proved to be effective in assessing residual stresses in laser beam welded aluminum alloys, allowing for accurate detection and characterization of stresses at different depths.
Effect of cold rolling on ultrasonic velocity and texture development in low carbon steel [1].	Timokhina, I., Hodgson, P., Ringer, S., Zheng, R., Pereloma, E.	2007	Cold rolling alters the ultrasonic velocity and texture of low carbon steel, providing insights into the microstructural changes occurring during the process.
Investigation on the influence of surface roughness on ultrasonic testing by numerical simulation and experiments [10].	Li, Y., Peng, Y., & Tian, G.	2021	Investigation of the influence of surface roughness on ultrasonic testing through numerical simulations and experiments, concluding that roughness affects the accuracy and reliability of ultrasonic testing.
Effect of surface roughness on ultrasonic wave propagation and attenuation in additive manufactured parts [11].	Muthulingam, S., Almajed, A., & Vairavan, R.	2021	Effect of surface roughness on ultrasonic wave propagation and attenuation in additive manufactured parts, concluding that roughness significantly influences the characteristics of ultrasonic waves.

Ultrasonic imaging based on amplitude and phase analysis for surface roughness measurement [12].	Zhang, J.; Zhou, Z.	2022	The technique demonstrated the ability to measure surface roughness with high precision, providing detailed information about surface topography through the analysis of amplitude and phase characteristics of ultrasonic signals.
Influence of surface roughness on ultrasonic nondestructive testing: A review [13].	Kaur, R., Sharma, P., & Singh, K.	2022	The review discusses the influence of surface roughness on nondestructive ultrasonic testing, providing an overview of the studies conducted so far.

In summary, these studies presented in the Table 1 demonstrate the potential of ultrasonic wave propagation techniques for their application in residual stress measurement.

## II. MATERIALS AND METHODS

### 2.1. Samples

In this present paper four steel samples named A, B, C and D were studied each three measuring points. All samples were prepared by machining using the milling and grinding processes, with selected cutting parameters, in order to result in surface topography as plane as possible and in two of them surface tensile residual stress as high as possible (sample C and D). To obtain high level of compressive residual stress shot peening treatment was carried out in machined surface in the sample A. In order to establish sample B as a stress-free reference, a stress relief heat treatment accomplished in a tubular furnace with controlled inert gas atmosphere to avoid decarbonation during heating, at 650°C, for two hours.

### 2.2. X-ray diffraction and ultrasonic techniques

For measurement of residual stresses by X-ray diffraction a Stresstech Xstress3000 analyzer (Figure 1) was selected using the  $\sin^2\psi$  method with radiation  $\text{CrK}\alpha$  ( $\lambda = 2.29092 \text{ \AA}$ ), diffracting the (211) plane of ferrite with a 2.0-mm diameter collimator (25 kV and 4.7 mA). Stresses were measured in longitudinal direction with achieved accuracy of approximately 15 MPa. The XTronic V1-0 Standard software (stresstechgroup.com) was used for the residual stress calculation. For ultrasound measurement was used Olimpkus pulse-receiver ultrasound equipment (Figure 2) with a pair of 10MHz and angular shoe of 70°, resulting in proper calibration of the Rayleigh wave signal.

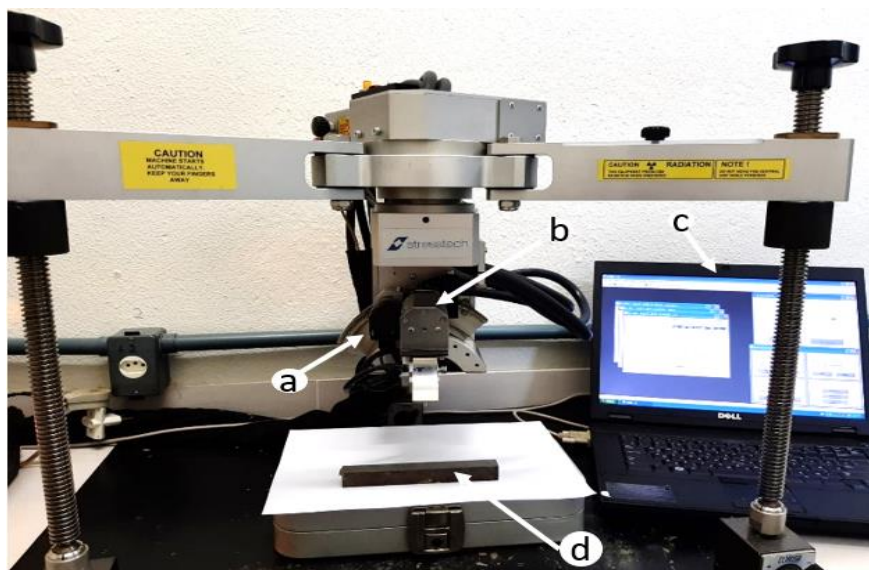
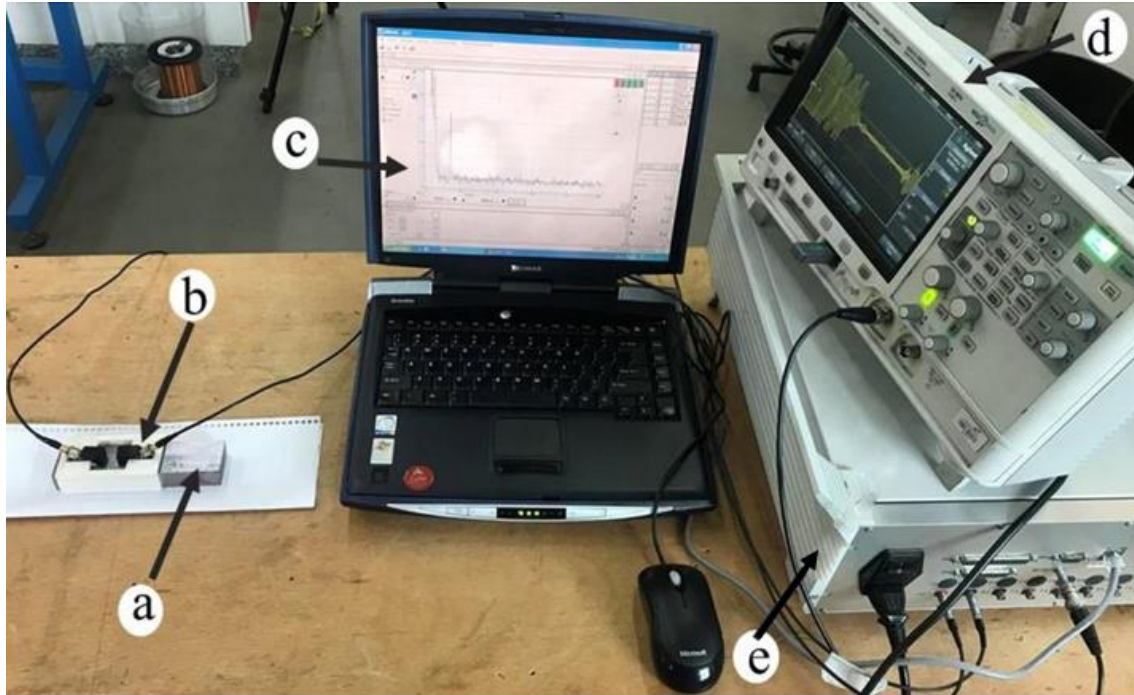


Figure 1. Stresstech Xstress3000 analyzer: a) goniometer, b) X-ray tube, c) software, d) sample.

For the ultrasonic measurements (Figure 2), in this experiment, the samples were machined to ensure the surfaces remained as parallel as possible. These limitations did not hinder the execution of the experiment, as a significant number of signals were collected per sample.

The 10 MHz frequency transducer performed effectively in generating amplitude vs. frequency and attenuation vs. frequency curves, consistent with previous findings [13].

To standardize the operation and facilitate result comparison, the following procedure was adopted during signal collection: the horizontal scale (time domain) of the ultrasound device was set to a range greater than the sample thickness, the gain used for scanning remained constant for all samples measured by the same pair of transducers and a sampling rate of 6000 Hz.



**Figure 2.** Pulse-receiver ultrasound equipment: a) sample, b) transducers, c) *software*, d) oscilloscope, e) signals generator.

For calculation of the attenuation ( $\alpha$ ), that is the ratio between signal amplitudes of reference sample and analyzed sample was necessary to compare the different frequency spectrum. Curve attenuation vs. frequency can be obtained adopting Eq. 1:

$$\alpha = \frac{1}{2t} \cdot 20\log(10) \cdot \frac{A_{reference}}{A_{analysis}} \quad (1)$$

where  $t$  denotes the sample thickness,  $A_{reference}$  the frequency spectrum of standard sample and  $A_{analysis}$  the frequency spectrum of analysis sample.

### III. RESULTS AND DISCUSSION

The analysis of residual stresses in all samples was conducted using the X-ray diffraction technique, which revealed varying levels and distributions of both tensile and compressive residual stresses intentionally induced during sample preparation. The corresponding Rayleigh wave values obtained for samples A and D, as presented in Table 2, aligned with the measured residual stress values. Notably, even among samples with the same nature of residual stresses but different magnitudes (such as A and D), discernible discrepancies in Rayleigh wave values were observed. This observation underscores the potential of this technique in accurately quantifying residual stress levels. In summary, these findings substantiate the utility of X-ray diffraction for residual stress analysis, facilitating the investigation of metallic materials' behavior under distinct stress conditions.

**Table 2.** Residual stresses measured by X-ray diffraction vs. time of flight.

Samples	Average Residual Stress (MPa)	Average time of flight ( $\mu$ s)
A	-450	0.110
B	350	0.160
C	390	0.170
D	10	0.140

The findings demonstrate that wave transit times in samples with tensile residual stresses (B and C) are higher in comparison to sample A, which exhibits a significant magnitude of compressive residual stress. Thus, it becomes feasible to compare these values with results obtained via X-ray diffraction. Based on the curves presented in Figure 3, it can be considered that the ultrasonic technique enables the quantification of residual stresses. This is particularly noteworthy as wave flight times in the material serve as a reliable indicator of the stress state present on the surface of structures and pipes, especially in field service conditions when access to laboratory facilities is limited. The application of the ultrasonic technique holds substantial potential for analyzing residual stresses in real-world settings, providing valuable insights into the assessment of structural integrity.

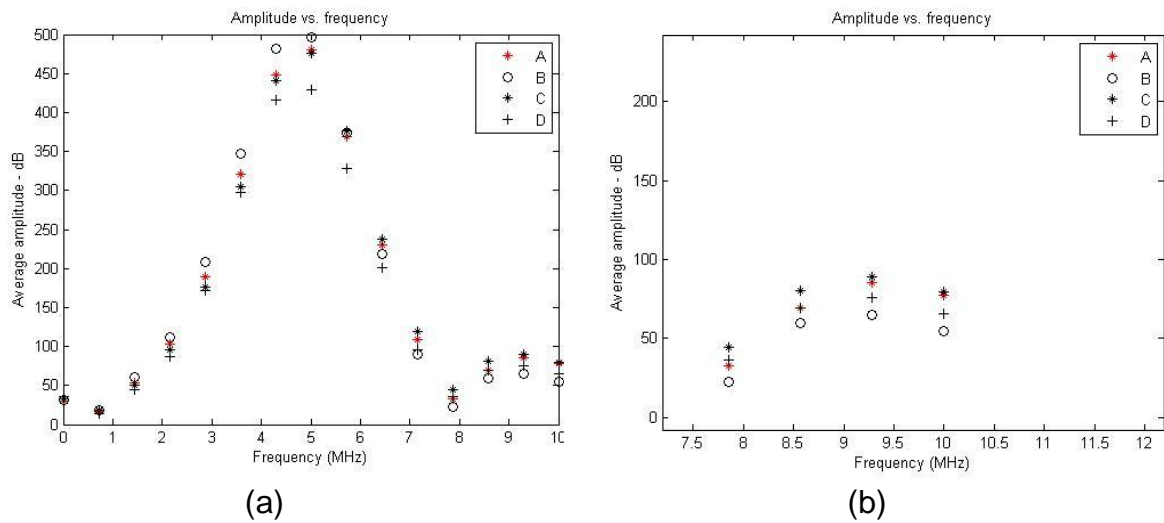


**Figure 3.** (a) Average Amplitude vs. Frequency. (b) Ultrasonic signal characterization for residual stresses.

Figure 3(a) illustrates that, at frequencies exceeding 2 MHz, the curves start to rise, with the maximum range for sample B observed between 4.94 and 5.05 MHz. The behavior of signal amplitudes in samples A and D is similar, but sample A demonstrates a higher magnitude of compressive residual stress, leading to a higher amplitude. Sample C exhibits a higher amplitude at 6 MHz, which decays as the frequency increases up to 9.5 MHz, as depicted in Figure 3(b).

Analyzing Figure 3(a), a similar behavior can be observed as reported by Khosravi and Ayoub [14] regarding the increase in ultrasonic signal amplitude with increasing frequency. This trend is explained by the increased interaction between the ultrasonic waves and the rough surface of the material.

The vertical bars in Figure 4(a) represent the standard deviation for each type of residual stress and (b), emphasizing the influence of X80 steel and residual stresses on sample behavior.

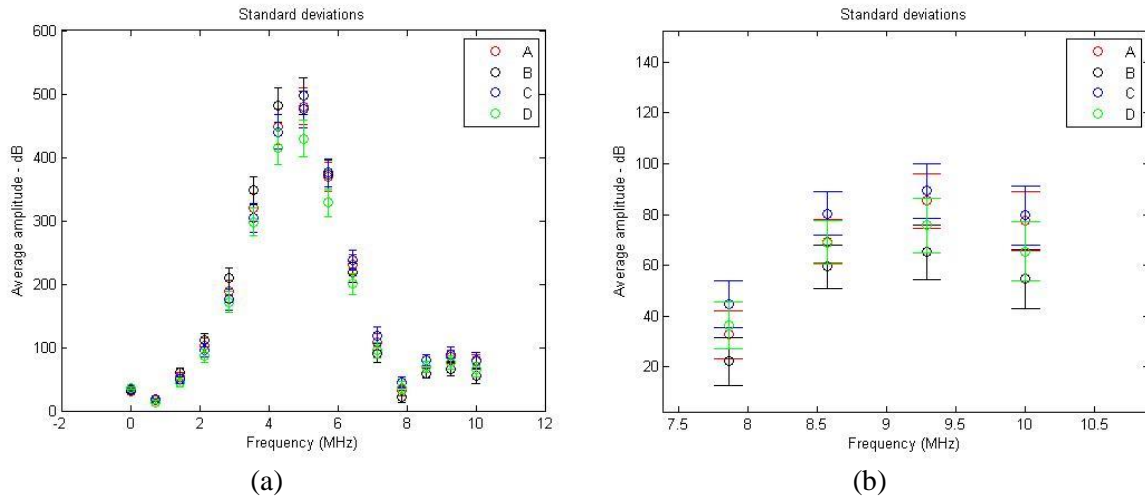


Figure 4. (a) Standard deviations. (b) Zoom region of 8 to 10 MHz at (a).

Differences in the behavior of samples with different types of residual stresses can be observed by analyzing the attenuation curves vs. frequency ( $\alpha \times f$ ). Sample C demonstrates tensile residual stress between 7 MHz and 8 MHz, while samples with compressive residual stress (A and D) exhibit distinct behavior, as shown in Figure 5(a) and (b).

The relationship between residual stress and ultrasonic technique has been investigated by several researchers. Timokhina *et al.* [1] examined the effect of cold rolling on ultrasonic velocity. Their study provides valuable insights into the relationship between residual stress and ultrasonic behavior in different samples. Testa *et al.* [2] assessed residual stress using ultrasonic testing and neutron diffraction, contributing to the understanding of the influence of residual stress on ultrasonic characteristics. De Camargo *et al.* [15] investigated the attenuation curves of samples with different types of residual stresses, further supporting the claim that the behavior of samples varies depending on the presence of tensile or compressive residual stress.

The standard deviations are displayed in Figure 6(a) and (b).

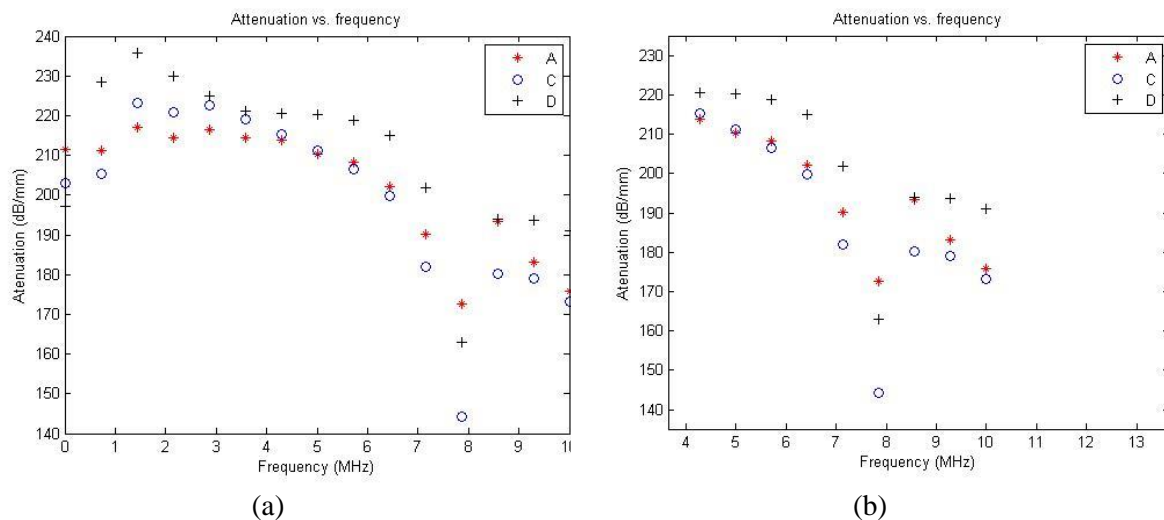


Figure 5. (a) Attenuation curves vs. frequency. (b) Residual stresses characterization.

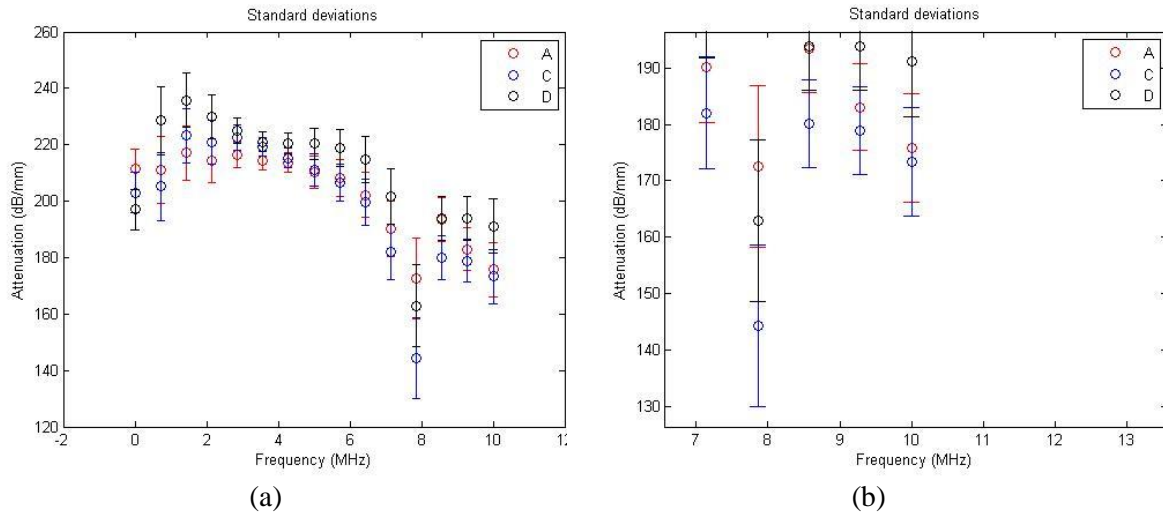


Figure 6. (a) Standard deviations. (b) Zoom region of 6 to 10 MHz at (a).

The presence of significant residual stresses in the steel samples affects the propagation of ultrasonic signals. Surface wave signals exhibit an inverse relationship between amplitude and attenuation, indicating that the deeper the Rayleigh wave (RW) penetrates into the strain layer containing residual stresses, the greater the observed attenuation. Furthermore, the attenuation vs. frequency curves ( $\alpha \times f$ ) presented in Figure 5(a) and (b) agree with the studies of Xu et al. [15] and Liu et al. [16] in relation to observed changes in attenuation due to surface roughness. The length of the ultrasonic wave is influenced by the used frequency, where higher frequencies affect only the surface layers, while lower frequencies penetrate deeper layers, corroborating the findings of Patel and Gandhi [17], in the research about the influence of surface roughness on the attenuation of ultrasonic waves and the relationship between the reduction in wave penetration and the residual stresses field. Likewise Seddik et al. [18], analyzing the application of ultrasonic techniques for measuring residual stresses, emphasized the importance of selecting an appropriate frequency that allows sufficient penetration in the material layers. By utilizing Equation 2 and the coefficients obtained from a calibration curve relating residual stresses and the RW parameter, we were able to calculate the residual stresses (Y) using the ultrasonic method, as illustrated in Figure 7(a) and (b).

Despite the low amplitude and sweep depth employed in this study, we observed less attenuation due to the reduced penetration depth into the strain layer containing residual stresses.

$$Y = a + bx + cx^2 \tag{2}$$

where  $a = 27.46$ ,  $b = -33.74$ ,  $c = 0.664$  and  $x = RW$ .

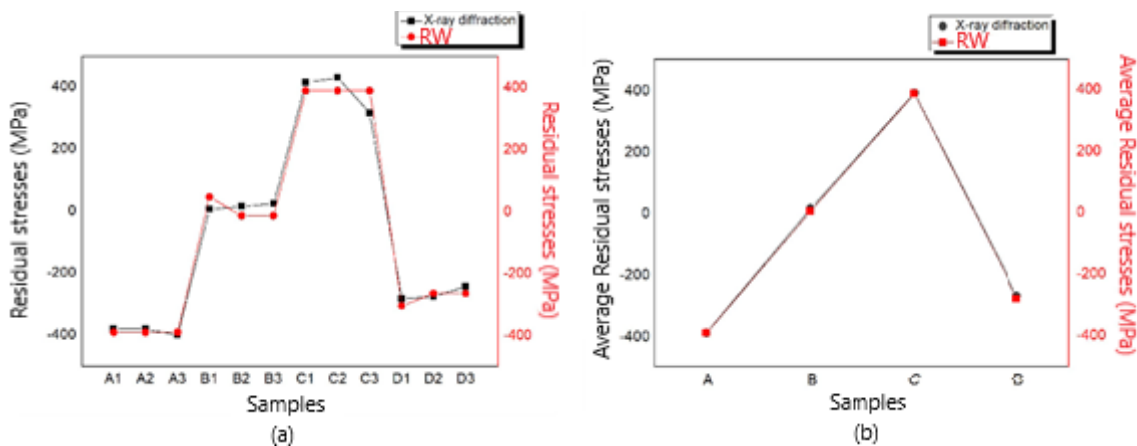
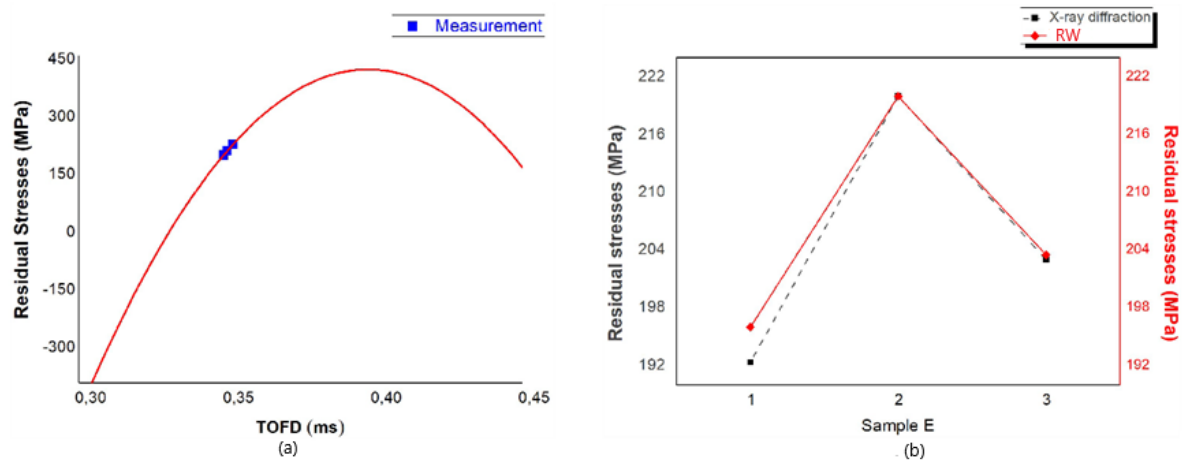


Figure 7. (a) Residual stresses. (b) Average residual stresses.

Analysis of Figure 7(a) and (b) indicates the successful measurement of residual stresses using the ultrasonic technique, with stress values similar to those obtained from the validation technique, X-ray diffraction, observed in all samples. To validate the ultrasonic technique, a calibration curve was

developed using the values of residual stress and times of flight of the Rayleigh wave. Figure 8(a) and (b) present the results of residual stresses in MPa for both non-destructive techniques, demonstrating the consistency between the results generated by the calibration curve and those obtained using X-ray diffraction.



**Figure 8.** (a) Calibration curve with residual stresses of the sample E. (b) Residual stress of sample E.

Measured RW (see Fig. 8(a)) shows that the measured RW in sample E are in the range of 0.35  $\mu$ s, all residual tensile stresses being in the order of 192 to 220 MPa (generated by the calibration curve) and in the range of 196 to 220 MPa (by the ultrasonic technique). Therefore, it can be stated that the calibration curve allows finding results are consistent with those of well-established techniques because all measured points of sample E showed converging residual stress, making it possible to perceive the potential of the ultrasonic technique for measurement of residual stress. The results of this study are in accordance with many studies (Zhang and Zhou [12], Muthulingam *et al.* [11], Ma and Zhou [19], Kaur *et al.* [20]) regarding the use of ultrasonic techniques for residual stress analysis, demonstrating that the ultrasonic technique is capable of quantifying residual stresses, providing results similar to those obtained through X-ray diffraction technique, as shown in Figure 7(a) and (b).

In summary, the results of this study corroborate and are consistent with the aforementioned previous studies, providing additional evidence on the influence of surface roughness on the propagation of ultrasonic waves and demonstrating the usefulness of the ultrasonic technique in residual stress analysis.

#### IV. CONCLUSIONS

For the results obtained in the present work, which aimed at the comparative study of residual stresses in X80 steel samples, by X-ray diffraction and using the ultrasonic technique, it was possible to obtain the following conclusions:

- 1) Wave times of flight in areas with compressive residual stresses are shorter than in those with tensile residual stress fields.
- 2) The spectrum frequency signal of the samples exhibited sensitivity in characterizing the residual stress patterns, and the attenuation curves allowed the characterization of signal behavior in samples with different stress levels, as the pattern of residual tensile stresses demonstrated the lowest attenuation.
- 3) Compared to the validated X-ray diffraction technique using a calibration curve, the RW ultrasonic technique demonstrates great potential for field application, enabling the qualification and quantification of residual stresses with promising results.

#### ACKNOWLEDGEMENT

This study was financed in part by the Coordenação de Aperfeiçoamento de Pessoal de Nível Superior - Brasil (CAPES) - Finance Code 001. The authors would also like to thank the Brazilian research agencies CNPq (304327/2021-2) and FAPERJ for the financial support.



## REFERENCES

- [1]. Timokhina, P. Hodgson, S. Ringer, R. Zheng, E. Pereloma, *Scr. Mater.* 44 (2007), 601-604. <https://doi.org/10.1016/j.scriptamat.2006.12.018>
- [2]. G. Testa, N. Bonora, D. Gentile, A. Ruggiero, G. Iannitti, A. Carlucci, Y. Madi, *Frat. Ed Integrità Strutt.* 11 (2017) 315–327. <https://doi.org/10.3221/IGF-ESIS.42.33>
- [3]. S. Kang, J. Speer, C. Van Tyne, T. Weeks, *Metals (Basel)*. 8 (2018) 354. <https://doi.org/10.3390/met8050354>
- [4]. L. Onyeji, G. Kale, *J. Mater. Eng. Perform.* 26 (2017) 5741–5752. <https://doi.org/10.1007/s11665-017-3031-x>
- [5]. G. Oliveira, M. Cindra Fonseca, A.C. Araujo, *Procedia CIRP* 77 (2018) 211–214. <https://doi.org/10.1007/s00170-017-0381-3>
- [6]. H.Y. Li, H.L. Sun, P. Bowen, J.F. Knott, *Int. J. Fatigue* 108 (2018) 53–61. <https://doi.org/10.1016/j.ijfatigue.2017.11.010>
- [7]. H.E. Coules, *Mater. Sci. Technol.* 29 (2013) 4–18. <https://doi.org/10.1016/j.matdes.2018.01.064>
- [8]. J. Wang, D. Zhang, B. Wu, M. Luo, *Mater. Res.* 20 (2017) 1681–1689. <http://doi.org/10.1590/1980-5373-mr-2017-0561>
- [9]. Li, Y., Peng, Y., & Tian, G. (2021). Investigation on the influence of surface roughness on ultrasonic testing by numerical simulation and experiments. *NDT & E International*, 124, 102366. <https://doi.org/10.1016/j.ndteint.2021.102366>
- [10]. Muthulingam, S., Almajed, A., & Vairavan, R. (2021). Effect of surface roughness on ultrasonic wave propagation and attenuation in additive manufactured parts. *Additive Manufacturing*, 42, 101957. <https://doi.org/10.1016/j.addma.2021.101957>
- [11]. Zhang, J., & Zhou, Z. (2022). Ultrasonic imaging based on amplitude and phase analysis for surface roughness measurement. *Measurement*, 187, 109970. <https://doi.org/10.1016/j.measurement.2021.109970>
- [12]. Singh, G., Pandey, S. K., & Kumar, P. (2020). Investigation of surface roughness effect on ultrasonic guided wave propagation in metallic plates. *Journal of Nondestructive Evaluation*, 39(1), 2. <https://doi.org/10.1007/s10921-019-00628-4>
- [13]. A. Lins, L.F.G. de Souza, M. Cindra Fonseca, *J. Mater. Eng. Perform.* 27 (2018) 124–137. <https://doi.org/10.3390/s17061449>
- [14]. N.S. Rossini, M. Dassisti, K.Y. Benyounis, A.G. Olabi, *Mater. Des.* 35 (2012) 572–588. <https://doi.org/10.1016/j.matdes.2011.08.022>
- [15]. A.K. Mondal, P. Biswas, S. Bag, *J. Mar. Sci. Appl.* 14 (2015) 250–260. <https://doi.org/10.1007/s11804-015-1320-z>
- [16]. S. Cong, W.W. Zhang, J.Y. Zhang, T. Gang, *Procedia Eng.* 207 (2017) 1910–1918. <https://doi.org/10.1016/j.proeng.2017.10.960>
- [17]. Khosravi, H., & Ayoub, A. (2020). The effect of surface roughness on ultrasonic testing in CFRP composites. *Composite Structures*, 230, 111554. <https://doi.org/10.1016/j.compstruct.2019.111554>
- [18]. P.C. De Camargo, S.E. Krüger, J.M.A. Rebello, *Scr. Mater.* 44 (2001) 2373–2378. [https://doi.org/10.1016/S1359-6462\(01\)00944-7](https://doi.org/10.1016/S1359-6462(01)00944-7)
- [19]. S. Zhang, X. Li, H. Jeong, *Sensors* 17 (2017) 1449. <https://doi.org/10.3390/s17061449>
- [20]. M.P. Arenas, R.M. Silveira, C.J. Pacheco, A.C. Bruno, J.F.D.F. Araujo, C.B. Eckstein, L. Nogueira, L.H. de Almeida, J.M.A. Rebello, G.R. Pereira, *J. Magn. Magn. Mater.* 456 (2018) 346–352. <https://doi.org/10.1016/j.jmmm.2019.165578>
- [21]. Xu, J., Tang, G., & Liu, J. (2020). Influence of roughness on ultrasonic guided wave propagation in aluminum plates. *Ultrasonics*, 108, 106192. <https://doi.org/10.1016/j.ultras.2020.106192>
- [22]. Liu, T., Zhang, Z., & Wang, W. (2020). Influence of surface roughness on ultrasonic guided wave propagation in steel plates. *Journal of Sound and Vibration*, 482, 115424. <https://doi.org/10.1016/j.jsv.2020.115424>
- [23]. V.D. Patel, A.H. Gandhi, *Measurement*. 138 (2019) 34–38. <https://doi.org/10.1016/j.measurement.2019.01.077>
- [24]. R. Seddik, M. Seddik, A. Atig, R. Fathallah, *Procedia Struct. Integr.* 2 (2016) 2182–2189. <https://doi.org/10.1016/j.prostr.2016.06.273>
- [25]. H. Huseynov, S. Abbas, *International Journal of Adv. Eng. & Tech.* (9) 2016 1-9.
- [26]. M. Huo, J. Zhao, H. Xie, Z. Li, S. Li, H. Zhang, Z. Jiang, *Wear* 426–427 (2019) 1286–1295. <https://doi.org/10.1016/j.wear.2018.12.053>
- [27]. X. Wu, S. Li, Z. Jia, B. Xin, X. Yin, *J. Mater. Process. Technol.* 268 (2019) 140–148. <https://doi.org/10.1007/s00170-020-05410-x>

- [28]. D. Gallitelli, V. Boyer, M. Gelineau, Y. Colaitis, E. Rouhaud, D. Retraint, R. Kubler, M. Desvignes, L. Barrallier, *Comptes Rendus Mécanique* 344 (2016) 355–374. <https://doi.org/10.1016/j.crme.2016.02.006>
- [29]. Ma, L., & Zhou, Z. (2020). Effects of surface roughness on ultrasonic wave scattering and backscattering intensity. *Journal of Sound and Vibration*, 486, 115574. <https://doi.org/10.1016/j.jsv.2020.115574>
- [30]. Kaur, R., Sharma, P., & Singh, K. (2022). Influence of surface roughness on ultrasonic nondestructive testing: A review. *Ultrasonics*, 112, 106491. <https://doi.org/10.1016/j.ultras.2021.106491>
- [31]. Li, L., Yang, L., & Zhang, H. (2020). The influence of operator technique on the accuracy of ultrasonic inspection for surface cracks. *Journal of Nondestructive Evaluation*, 39(1), 14. <https://doi.org/10.1007/s10921-019-0621-5>
- [32]. Chouaib, N., Breitkopf, P., & Duquennoy, M. (2021). Experimental and numerical investigation of the influence of surface roughness on ultrasonic guided waves in complex structures. *Journal of Sound and Vibration*, 506, 116375. <https://doi.org/10.1016/j.jsv.2021.116375>
- [33]. Abuhmaidan, M. H., & Chauhan, S. (2021). Experimental investigation on the influence of surface roughness on guided wave propagation in composite plates. *Composite Structures*, 255, 113191. <https://doi.org/10.1016/j.compstruct.2020.113191>
- [34]. Fan, Y., & He, C. (2022). Experimental study on the influence of surface roughness on guided wave propagation in steel plates. *Journal of Sound and Vibration*, 534, 116334. <https://doi.org/10.1016/j.jsv.2021.116334>
- [35]. Joshi, M., Manjula, S. H., & Basavarajappa, S. (2021). Experimental investigation on the effect of surface roughness on ultrasonic guided waves in carbon fiber-reinforced polymer composites. *Ultrasonics*, 112, 106468. <https://doi.org/10.1016/j.ultras.2021.106468>
- [36]. Li, Y., Guo, Z., & Liu, W. (2021). Effect of surface roughness on guided wave propagation in composite plates: A numerical and experimental investigation. *Composite Structures*, 267, 114401. <https://doi.org/10.1016/j.compstruct.2021.114401>

## AUTHORS

**Maria Cindra** holds a Bachelor's and Master's degree in Mechanical Engineering from the University of Friendship of Peoples (Moscow, Russia, 1985) and a Ph.D. in Metallurgical and Materials Engineering from the Federal University of Rio de Janeiro (PEMM/COPPE/UFRJ, 2000). She is a Full Professor at UFF - Federal Fluminense University, working in the Department of Mechanical Engineering and the Graduate Program in Mechanical Engineering. She is the coordinator of the Laboratory of Stress Analysis (LAT/UFF). Her expertise lies in the fields of Mechanical Engineering and Metallurgical and Materials Engineering, with a focus on Residual Stress Analysis by X-ray Diffraction Technique, Mechanical Manufacturing Processes, and Mechanical Properties of Metals and Alloys.



**Bruna Machado** holds a Bachelor's degree in Mechanical Engineering from CEFET/RJ and a Master's degree in Mechanical Engineering from the Federal Fluminense University. Currently, she is pursuing a Ph.D. in Mechanical Engineering at UFF. Bruna has worked as a professor in the Mechanical Engineering department at CEFET/RJ during both semesters of 2020, and in the Mechanical Engineering department at UERJ between 2022 and 2023, where she taught courses in Metallography and Heat Treatments I and II. Her expertise lies in the field of Mechanical Engineering, with a focus on Manufacturing processes and Analysis of Residual Stresses using X-ray Diffraction, Conventional Ultrasonics and TOFD, as well as Magnetic Barkhausen Noise



**Gabriela Ribeiro** holds a Bachelor's degree in Physics with a specialization in Medical Physics from the Federal University of Rio de Janeiro (2004), a Master's degree (2006), and a Ph.D. in Nuclear Engineering from the Federal University of Rio de Janeiro (2010). She is currently an Associate Professor in the Metallurgical and Materials Engineering Program (PEMM) at COPPE/UFRJ. She is the Head of the Non-Destructive Testing area within the Metallurgical and Materials Engineering Program (PEMM) and is affiliated with the Laboratory of Non-Destructive Testing, Corrosion, and Welding (LNDC). She is an affiliate member of the Brazilian Academy of Sciences. Her expertise lies in the field of Materials Engineering and Metallurgy, with a focus on Non-Destructive Testing, primarily in the areas of Ultrasonics,



Phased Array, Thermography, Magnetic Testing, Radiography, X-ray Transmission Microtomography, PoD, and sensor development. She has published over 40 papers in indexed international journals. Her research is focused on the development of inspection methodologies and the study of non-destructive techniques for structural evaluation and characterization of different materials used in the industry.

**Mauricio Motta** holds a Bachelor's degree in Mechanical Industrial Engineering from the Federal Center for Technological Education Celso Suckow da Fonseca (1987), a Master's degree in Metallurgical and Materials Engineering from the Federal University of Rio de Janeiro (1993), and a Ph.D. in Metallurgical and Materials Engineering from the Federal University of Rio de Janeiro (2000). He is currently the Director-General and Full Professor at the Federal Center for Technological Education Celso Suckow da Fonseca. His expertise lies in the field of Materials Engineering and Metallurgy, with a focus on Ultrasonics, primarily in the areas of ultrasonics, non-destructive testing, materials characterization, and failure analysis.

